41. Dane MJ, Khairoun M, Lee DH *et al.* Association of kidney function with changes in the endothelial surface layer. *Clin J Am Soc Nephrol* 2014; 9: 698–704
42. Johnson RJ, Herrera-Acosta J, Schreiner GF *et al.* Subtle acquired renal injury as a mechanism of salt-sensitive hypertension. *N Engl J Med* 2002; 346: 913–923
43. Boudville N, Ward S, Benaroia M *et al.* Increased sodium intake correlates with greater use of antihypertensive agents by subjects with chronic kidney disease. *Am J Hypertens* 2005; 18: 1300–1305
44. Miyakawa H, Woo SK, Dahl SC *et al.* Tonicity-responsive enhancer binding protein, a rel-like protein that stimulates transcription in response to hypertonicity. *Proc Natl Acad Sci USA* 1999; 96: 2538–2542
45. Choi SY, Lim SW, Salimi S *et al.* Tonicity-responsive enhancer-binding protein mediates hyperglycemia-induced inflammation and vascular and renal injury. *J Am Soc Nephrol* 2018; 29: 492–504
46. Choi S, You S, Kim D *et al.* Transcription factor NFAT5 promotes macrophage survival in rheumatoid arthritis. *J Clin Invest* 2017; 127: 954–969
47. Remo A, Simeone I, Pancione M *et al.* Systems biology analysis reveals NFAT5 as a novel biomarker and master regulator of inflammatory breast cancer. *J Transl Med* 2015; 13: 138
48. Roth I, Leroy V, Kwon HM *et al.* Osmoprotective transcription factor NFAT5/TonEBP modulates nuclear factor-κB activity. *Mol Biol Cell* 2010; 21: 3459–3474

*Received: 21.10.2018; Editorial decision: 11.2.2019*

ORIGINAL ARTICLE

Nephrol Dial Transplant (2019) 34: 2042–2050
doi: 10.1093/ndt/gfz050
Advance Access publication 10 April 2019

# Fibroblast-specific plasminogen activator inhibitor-1 depletion ameliorates renal interstitial fibrosis after unilateral ureteral obstruction

Lan Yao[1,2,*], M. Frances Wright[1,*], Brandon C. Farmer[1,3], Laura S. Peterson[1], Amir M. Khan[1,4], Jianyong Zhong[1,5], Leslie Gewin[6], Chuan-Ming Hao[7], Hai-Chun Yang[1,5] and Agnes B. Fogo[1,5,6]

[1]Department of Pathology, Microbiology, and Immunology, Vanderbilt University Medical Center, Nashville, TN, USA, [2]Medical Healthcare Center, Beijing Friendship Hospital of Capital Medical University, Beijing, China, [3]Department of Biology, Western Kentucky University, Bowling Green, KY, USA, [4]Chicago Medical School at Rosalind Franklin University of Medicine and Science, North Chicago, IL, USA, [5]Division of Pediatric Nephrology, Vanderbilt University Medical Center, Nashville, TN, USA, [6]Division of Nephrology, Vanderbilt University Medical Center, Nashville, TN, USA and [7]Division of Nephrology, Huashan Hospital, Fudan University, Shanghai, China

Correspondence and offprint requests to: Agnes B. Fogo; E-mail: agnes.fogo@vanderbilt.edu
*These authors contributed equally to this work.

## ABSTRACT

**Background.** Plasminogen activator inhibitor-1 (PAI-1) expression increases extracellular matrix deposition and contributes to interstitial fibrosis in the kidney after injury. While PAI-1 is ubiquitously expressed in the kidney, we hypothesized that interstitial fibrosis is strongly dependent on fibroblast-specific PAI-1 (fbPAI-1).

**Methods.** Tenascin C Cre (TNC Cre) and fbPAI-1 knockdown (KD) mice with green fluorescent protein (GFP) expressed within the TNC construct underwent unilateral ureteral obstruction and were sacrificed 10 days later.

**Results.** $GFP^+$ cells in fbPAI-1 KD mice showed significantly reduced PAI-1 expression. Interstitial fibrosis, measured by Sirius red staining and collagen I western blot, was significantly decreased in fbPAI-1 KD compared with TNC Cre mice. There was no significant difference in transforming growth factor β (TGF-β) expression or its activation between the two groups. However, $GFP^+$ cells from fbPAI-1 KD mice had lower TGF β and connective tissue growth factor (CTGF) expression. The number of fibroblasts was decreased in fbPAI-1 KD compared with TNC Cre mice, correlating with decreased alpha smooth muscle actin (α-SMA) expression and less fibroblast cell proliferation. TNC Cre mice had decreased E-cadherin, a marker of differentiated tubular epithelium, in contrast to preserved expression in fbPAI-1 KD. F4/80-expressing cells, mostly $CD11c^+/F4/80^+$ cells, were increased while M1 macrophage markers were decreased in fbPAI-1 KD compared with TNC Cre mice.

**Conclusion.** These findings indicate that fbPAI-1 depletion ameliorates interstitial fibrosis by decreasing fibroblast proliferation in the renal interstitium, with resulting decreased collagen I. This is linked to decreased M1 macrophages and preserved tubular epithelium.

**Keywords:** fibroblast, interstitial fibrosis, PAI-1

## INTRODUCTION

Tubulointerstitial fibrosis represents a final common pathway for many etiologies of chronic kidney disease, which is a worldwide public health problem and a heavy burden on the healthcare system [1]. Renal prognosis strongly correlates with the degree of tubulointerstitial fibrosis [2]. Elucidating the pathophysiology of tubulointerstitial fibrosis and approaches to mitigate or reverse it therefore has significant therapeutic potential.

Plasminogen activator inhibitor-1 (PAI-1) is a member of the serine protease inhibitor family that inhibits fibrinolysis by interfering with urokinase-type plasminogen activator and tissue-type plasminogen activator–mediated degradation of extracellular matrix (ECM) and fibrin. Additionally, PAI-1 influences cellular migration through interactions with its cofactor vitronectin as well as the urokinase receptor and its coreceptors [3]. Healthy kidneys express low levels of PAI-1, but many different renal cell types and infiltrating cells produce abundant levels of PAI-1 in both acute and chronic disease states [3, 4]. Increased PAI-1 is implicated in renal fibrosis in the setting of both glomerular and interstitial disease, and in both animals and humans [5–7]. Genetic PAI-1 deficiency or pharmaceutical anti-PAI-1 therapy is protective in various models, including diabetic nephropathy, 5/6 nephrectomy, protein overload and the unilateral ureteral obstruction (UUO) model of interstitial fibrosis [3, 8, 9]. UUO-induced renal fibrosis was attenuated in PAI-$1^{-/-}$ mice, associated with decreased interstitial myofibroblasts and macrophages [10]. In contrast, PAI-1-overexpressing mice showed more interstitial fibrosis after UUO [11].

In the setting of renal injury, many different cell types express PAI-1 and contribute to fibrosis; however, the relative contributions of particular cell types are unknown. Fibroblasts are considered the main cells that synthesize many key components of the ECM, including collagen types I, III and V and fibronectin, as well as matrix-degrading proteases [2]. Given the involvement of fibroblasts in ECM accumulation after injury and the promotion of fibrosis by increased systemic PAI-1, fibroblasts represent an attractive target for PAI-1 knockdown (KD). In this study, we investigated the effects of fibroblast-specific PAI-1 (fbPAI-1) KD in the tubulointerstitial fibrosis model of UUO.

## MATERIALS AND METHODS

### Experimental design and animals

PAI-$1^{loxp/loxp}$ and wild-type mice were crossed with mice with Cre driven by the tenascin C (TNC) promoter TNC-Cre/ERT [12]. Green fluorescent protein (GFP) is expressed with this TNC construct, which allows tracking $TNC^+$ cells by GFP staining. Mice were further crossed with the mT/mG reporter mouse to evaluate the Cre efficiency (Jackson Laboratory, Bar Harbor ME, USA). UUO was performed as previously reported in PAI-$1^{loxp/loxp}$/TNC Cre mice (fbPAI-1 KD, $n = 11$) and control wild-type/TNC Cre mice (TNC Cre, $n = 8$) at the age of 10 weeks after treatment with tamoxifen over the preceding 10 days (4 mg 5× intraperitoneally every other day) [13]. Mice were sacrificed 10 days after UUO.

### Immunohistochemistry

Kidney tissue was fixed in 4% paraformaldehyde and paraffin-embedded and 3-μm thick sections were cut. For staining of F4/80, sections were trypsinized (1 mg/mL; Sigma Aldrich, St Louis, MO, USA) for 20 min at 37°C. For fibroblast-specific protein-1 (FSP-1) and α-smooth muscle actin (α-SMA) staining, sections were heated in 0.01 mol/L sodium citrate buffer for 10 min. Endogenous peroxidase was quenched with 3% hydrogen peroxidase for 10 min and slides were exposed to Power Block (BioGenex Laboratories, San Ramon, CA, USA) for 30 min. Sections were incubated with the following primary antibodies: rabbit anti-mouse FSP-1 (1:400; Abcam, Cambridge, MA, USA), mouse anti-mouse α-SMA (1:800; Agilent, Santa Clara, CA, USA) or rat anti-mouse F4/80 (1:800; AbD Serotec, Raleigh, NC, USA) overnight at 4°C. Immunoperoxidase staining was performed with the Vectastain ABC kit (Vector Laboratories, Burlingame, CA, USA), with diaminobenzidine (DAB) as a chromogen. Hematoxylin was used as a counterstain. Negative controls done without primary antibody showed no staining and known positive controls stained appropriately. FSP-$1^+$ cells were counted in 40 high power fields (HPFs; 40×) per mouse. α-SMA was quantified by the percentage of positive area in 40 HPFs (40×).

Double-staining for proliferating cell nuclear antigen (PCNA) and α-SMA was done using citrate buffer for antigen retrieval and the M.O.M. Kit (Vector Laboratories) to block, followed by mouse anti-mouse PCNA (1:400; Agilent) at 4°C overnight. The second antibody used ImmPRESS reagent (Vector Laboratories) with DAB as a chromogen. Sections were then incubated with mouse anti-mouse α-SMA (1:400) at 37°C for 1 h, followed by anti-mouse horseradish peroxidase (HRP) (ImmPRESS reagent) and ImmPACT VIP substrate (Vector Laboratories). Omitting antibody to PCNA or α-SMA or both was used for negative controls. $PCNA^+$/ α-$SMA^+$ cells were counted in 40 high power fields (20X) per mouse.

Double-staining for GFP and PAI-1 was also done with ethylenediaminetetraacetic acid buffer (Abcam) for antigen retrieval and the M.O.M. Kit (Vector Laboratories) to block, followed by goat anti-mouse GFP (1:200; Abcam) at 4°C overnight. The second antibody used anti-goat HRP (ImmPRESS reagent) and Alexa Fluor 488 Tyamide SuperBoost (Life Technologies, Carlsbad, CA, USA). Sections were incubated with mouse anti-mouse PAI-1 (1:500; BD Biosciences, San Jose, CA, USA) at 4°C overnight, followed by anti-mouse HRP (ImmPRESS reagent) and Alexa Fluor 555 Tyamide SuperBoost (Life Technologies).

### Periodic acid–Schiff and Sirius red staining

Tubular injury was examined on periodic acid–Schiff and Masson's trichrome–stained slides. Tubular injury was scored in the cortex of the obstructed kidney per HPF, averaging all fields, as follows: 0 = no injury, 1 = 1–25% of area injured, 2 = 26–50%, 3 = 51–75% and 4 = 76–100%. Tubular injury was defined as sloughing of tubular epithelial cells, tubular cast formation, tubular dilatation or tubular atrophy.

For quantitative assessment of tubulointerstitial fibrosis, sections were stained with Picro-Sirius red (0.1% Sirius red in

saturated picric acid) for 16 h, followed by washing with 0.5% acetic acid twice. Sections were examined by polarized light microscopy. The Sirius red–positive polarized area in the cortex was measured by image analyzing software (Axiovision, Carl Zeiss, Thornwood, NY USA) and presented as percentage positive area of total cortex.

### Western blot

Frozen kidney samples were homogenized in radioimmunoprecipitation assay buffer containing proteinase inhibitor (Roche Diagnostics, Mannheim, Germany) and phosphatase inhibitor (Sigma-Aldrich). The protein concentration was measured using a Dc Protein Assay kit (Bio-Rad Laboratories, Hercules, CA, USA). Samples were separated on 10% sodium dodecyl sulfate–polyacrylamide gel electrophoresis and transferred onto a 0.2 µmol/L nitrocellulose membrane. Collagen I (1:1000; Abcam), E-cadherin (1:400; Abcam) and P-Smad3 (1:400; Cell Signaling Technology, Danvers, MA, USA) were detected by the corresponding antibody overnight at 4°C. After washing in Tris-buffered saline with 0.1% Tween-20 (TBS-T), the species-appropriate HRP-labeled secondary antibody (1:2500 in 5% non-fat milk TBS-T) was added and incubated at room temperature for 1 h. Protein bands on western blots were visualized by ECL Plus (Amersham, Arlington Heights, IL, USA) according to the manufacturer's instructions and developed on film. The membranes were stripped with 100 mmol/L β-mercaptoethanol, 2% sodium dodecyl sulfate and 62.5 mmol/L Tris-HCl at pH 6.7. The amount of protein loading was detected by using mouse anti-β-actin monoclonal antibody (1:10 000; Sigma-Aldrich).

### Flow cytometry and macrophage isolation

The obstructed and contralateral kidneys from four TNC Cre and four fbPAI-1 KD mice were minced and incubated with 2 mg/mL collagenase II (Sigma-Aldrich), 1 mL Dulbecco's modified Eagle's medium and 10 µl/mL DNAse (Bio-Rad Laboratories) at 37°C for 1 h. The tissue was filtered using 70 µm and then 40 µm sieves and incubated with red blood cell lysis buffer at 37°C for 5 min, neutralized with phosphate-buffered saline (PBS), centrifuged and resuspended in PBS with 0.5% fetal bovine serum (FBS). For flow analysis of cell surface protein expression, samples were incubated with Fc blocking antibody (Biolegend, San Diego, CA, USA) on ice for 10 min. Samples were then incubated with phycoerythrin-conjugated anti-F4/80, allophycocyanin (APC)-conjugated anti-CD11c or the appropriate APC-conjugated isotype controls (Biolegend) for 30 min at room temperature. Cells were analyzed on an FACSCanto II cytometer with FACSDiva software (BD Biosciences) for data acquisition and analysis.

Tissues from additional TNC Cre and fbPAI-1 KD mice ($n = 8$ and 11, respectively) were minced, digested and filtered as detailed above. Cells were resuspended and incubated with CD11b or GFP selective reagent (Stemcell Technologies, Cambridge, MA, USA). Macrophage ($CD11b^+$) and TNC-expressing ($GFP^+$) cells were isolated using the EasyEights magnetic cell separation system (Stemvell Technologies), following the manufacturer's instructions [14]. RNA was isolated using an RNeasy Mini Kit (Qiagen, Germantown, MD, USA).

### Quantitative real-time polymerase chain reaction (PCR)

Reverse transcription was performed using the High-Capacity cDNA Reverse Transcription Kit (Applied Biosystems, Branchburg, NJ, USA). Quantitative real-time PCR was performed in a total reaction volume of 25 µL using 12.5 µL Universal Master Mix II, 1.25 µL forward and reverse primers [PAI-1, collagen I, transforming growth factor β (TGF-β), CTGF, α-SMA, E-cadherin, inducible nitric oxide synthase (iNOS), Chemokine (C-C motif) ligand 3 (Ccl3), CD86, CD38, arginase 1, Ym-1, CD206 and Egr2] (Life Technologies) and 11.25 µL cDNA (5 ng/µL). Quantitative real-time PCR was carried out using the CFX96 Real-Time PCR Detection System (Bio-Rad Laboratories) with the following cycling parameters: polymerase activation for 10 min at 95°C and amplification for 40 cycles of 15 s at 95°C and 60 s at 60°C. Experimental cycle threshold ($C_t$) values were normalized to 18S measured on the same plate, and fold differences in gene expression were determined by using the $2^{-\triangle\triangle Ct}$ method [15].

### Statistical analysis

Results are expressed as mean ± standard error of the mean (SEM). Statistical differences were assessed by Student's *t*-test with unequal variance. Nonparametric data were compared by Mann–Whitney U-test. P-values $<0.05$ were considered to be significant.

## RESULTS

### fbPAI-1 KD reduces PAI-1 expression in fibroblasts

We first verified TNC-Cre activity by crossing these mice with the mT/mG reporter, which has ubiquitous membrane-bound red fluorescence (Figure 1A, left panel) to green that is converted to green (GFP) (Figure 1A, right panel) by Cre activity [16]. In the uninjured TNC Cre mice, Cre activity was detected in peritubular cells primarily in the medullary interstitium, with very few positive cells in the cortex (Figure 1A and Supplementary data, Figure S1A). Since TNC Cre is located on fibroblasts and is labeled by GFP by this construct, we next identified GFP and PAI-1 colocalization by double-staining. At Day 10 after UUO in obstructed kidneys in fbPAI-1 KD mice, ∼80% of GFP-positive cells were PAI-1 negative while TNC Cre mice showed PAI-1 positivity in all interstitial fibroblast-type (GFP-positive) cells (Figure 1B and Supplementary data, Figure S1B). Next, we isolated $GFP^+$ cells from both contralateral nonobstructed and obstructed kidneys. $GFP^+$ cells derived from obstructed kidneys had >20-fold higher PAI-1 expression versus contralateral nonobstructed kidneys in TNC Cre mice. In contrast, in fbPAI-1 KD mice, both obstructed and contralateral nonobstructed kidneys showed a significant reduction of PAI-1 expression compared with TNC Cre mice (Figure 1C). These results demonstrate the efficiency of our fbPAI-1 KD model in achieving PAI-1 depletion.

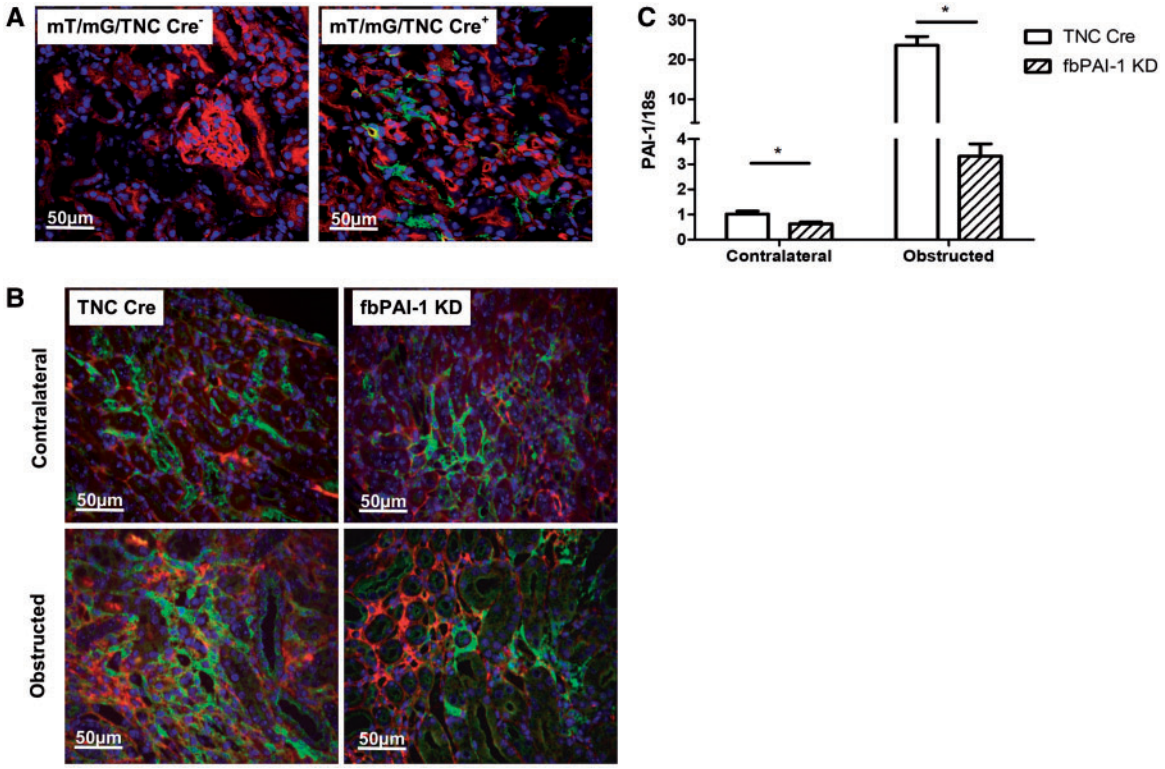


**FIGURE 1:** Effective fibroblast-specific KD of PAI-1. (**A**) The mT/mG mouse was crossed with TNC-Cre-expressing mice, where Cre activity converts ubiquitous membrane-bound red fluorescence (left panel) to green (right panel). (**B**) Kidney sections were double-stained for PAI-1 (red) and GFP (green). About 76–87% of GFP-positive cells, i.e. fibroblasts, were PAI-1 negative in fbPAI-1 KD mice. Obstructed kidneys from TNC Cre mice showed increased PAI-1 expression and all interstitial $GFP^+$ cells expressed PAI-1 in these mice. (**C**) PAI-1 mRNA level was less in isolated $GFP^+$ cells from fbPAI-1 KD versus TNC-Cre mice. *$P < 0.05$.

### fbPAI-1 KD reduces interstitial fibrosis

At Day 10 after UUO, Sirius red staining showed significantly less collagen in fbPAI-1 KD mice compared with TNC Cre ($0.87 \pm 0.10$ versus $1.33 \pm 0.14\%$, $P < 0.05$) (Figure 2A). Likewise, levels of collagen I protein and mRNA ($0.59 \pm 0.10$ versus $1.23 \pm 0.29$, $P < 0.05$) were significantly decreased in the obstructed kidneys of fbPAI-1 KD compared with TNC Cre (Figure 2B). PAI-1 mRNA expression was decreased by 42% in fbPAI-1 KD kidneys compared with TNC Cre after UUO (Figure 2C; $P < 0.05$). Of note, there was no kidney difference in either TGF-β mRNA expression (fbPAI-1 KD $1.23 \pm 0.18$ versus TNC Cre $1.06 \pm 0.14$, $P > 0.05$) or phosphorylated Smad3 protein (fbPAI-1 $0.90 \pm 0.21$ versus TNC Cre $1.40 \pm 0.44$, $P > 0.05$), a marker of TGF-β signaling activation, in mice with fibroblast-specific KD versus intact PAI-1 (Supplementary data, Figure S2). However, in isolated fibroblasts ($GFP^+$ cells) from obstructed kidneys, TGF-β and CTGF expressions were reduced in fbPAI-1 KD versus TNC Cre (Figure 2D).

### fbPAI-1 KD reduces myofibroblasts

At Day 10 after UUO, FSP-1 immunostaining revealed significantly fewer fibroblasts in fbPAI-1 KD versus TNC Cre mice ($21.33 \pm 1.66$ versus $31.81 \pm 1.11$ FSP-1-positive cells/HPF, $P < 0.05$) (Supplementary data, Figure S3). FbPAI-1 KD mice also showed significantly less interstitial α-SMA positivity compared with TNC Cre ($8.86 \pm 0.51\%$ versus $11.13 \pm 0.60\%$, $P < 0.05$) (Figure 3A). Furthermore, $GFP^+$ cells isolated from obstructed kidneys showed less α-SMA expression in fbPAI-1 KD versus TNC Cre (Figure 3B). *In vivo*, PCNA/α-SMA double-staining demonstrated significantly less fibroblast proliferation in fbPAI-1 KD compared with TNC Cre ($0.85 \pm 0.15$ versus $1.53 \pm 0.13$, $P < 0.05$) (Figure 3C).

### fbPAI-1 KD ameliorates tubular injury

fbPAI-1 KD mice showed less tubular injury, with less sloughing of tubular epithelial cells, tubular cast formation, tubular dilatation and tubular atrophy versus TNC Cre mice (Figure 4A). Both E-cadherin mRNA, measured by real-time PCR, and protein levels, measured by Western blot, were higher in fbPAI-1 KD compared with TNC Cre mice (Figure 4B), indicating less tubular epithelial cell injury in fbPAI-1 KD mice after UUO.

### fbPAI-1 KD and macrophages

F4/80 staining at Day 10 after UUO revealed significantly more interstitial F4/80-positive cells in fbPAI-1 KD compared with TNC Cre mice ($32.86 \pm 1.07$ versus $23.30 \pm 1.78$/HPF, $P < 0.05$) (Figure 5A). F4/80 is expressed on both dendritic cells and macrophages. We therefore assessed both CD11c and F4/80 to determine the specific inflammatory cells increased in the fbPAI-1 KD kidneys. Additional studies by flow cytometry confirmed more $F4/80^+$ cells in fbPAI-1 KD than TNC Cre mice kidneys after UUO. $CD11c^+/F4/80^-$ dendritic cells were

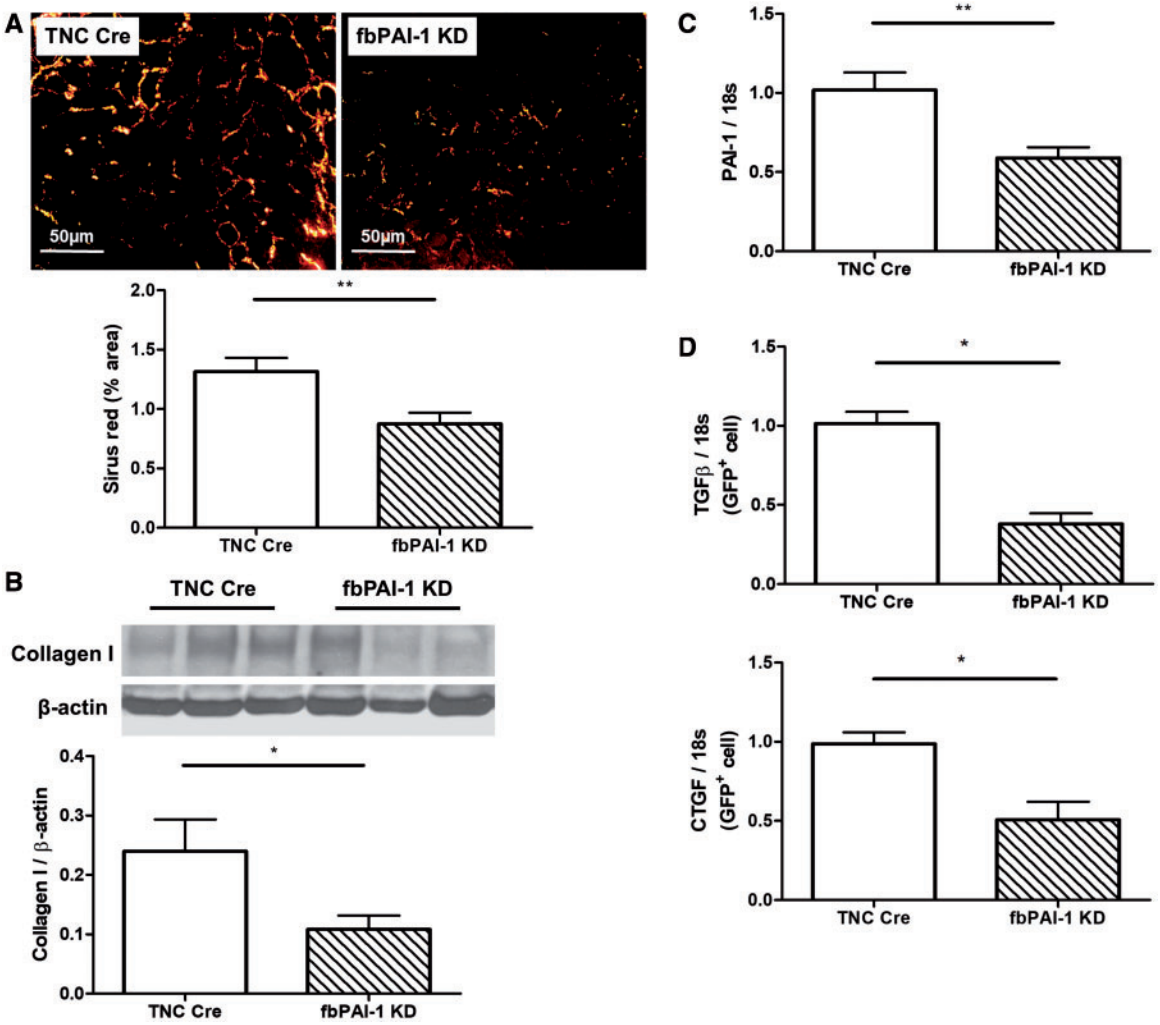


FIGURE 2: Decreased interstitial fibrosis in fbPAI-1 KD mice. (**A**) Polarized Sirius red positivity, a marker of collagen, was less in fbPAI-1 KD kidney versus TNC Cre 10 days post-UUO. (**B**) Collagen 1 protein levels were decreased in obstructed kidneys of fbPAI-1 KD versus TNC Cre at Day 10. (**C**) Renal PAI-1 expression was reduced in fbPAI-1 KD versus TNC Cre. (**D**) $GFP^+$ cells derived from fbPAI-1 KD showed less TGF-β and CTGF expression. $^*P < 0.05$, $^{**}P < 0.01$.

similar in the two groups. $CD11c^+/F4/80^+$ macrophage/dendritic cells, but not $CD11c^-/F4/80^+$ macrophages, were significantly increased in fbPAI-1 KD kidneys (Figure 5B). To further characterize the polarization of renal macrophages, we isolated renal $CD11b^+$ macrophages/dendritic cells and assessed markers of M1 versus M2 macrophages. Macrophage transcript levels of M1-associated genes (iNOS, Ccl3, CD86 and CD38) were reduced in cells from obstructed kidney of fbPAI-1 KD versus TNC Cre. CD206 and Egr2, two M2 markers, were also reduced in fbPAI-1 KD kidneys while arginase-1 and Ym-1, two additional M2 markers, showed no difference between the two groups (Figure 5C).

## DISCUSSION

Our study demonstrates that depleting PAI-1 in renal fibroblasts attenuates renal fibrosis after UUO, manifested by decreased collagen I, fewer fibroblasts and less fibroblast proliferation. Additionally, fbPAI-1 KD resulted in increased $CD11c^+/F4/80^+$ cells and decreased M1 macrophage expression after UUO.

Multiple previous studies have shown that inhibiting systemic PAI-1 ameliorates renal interstitial fibrosis [10, 11]. In the kidney, PAI-1 is produced and secreted by multiple resident cell types, but it is unclear which cell types are responsible for PAI-1-dependent fibrosis. Here we report that fbPAI-1 depletion is sufficient to mitigate interstitial fibrosis, suggesting that renal fibroblast-derived PAI-1 plays an important role in tubulointerstitial fibrosis.

The reduced fibrosis in PAI-1 conditional KD mice is likely due to reduced myofibroblast numbers. Studies indicate that the origin of myofibroblasts after renal injury could be contributed to by proliferating resident renal fibroblasts, pericytes, bone marrow–derived cells, endothelial–mesenchymal transition or epithelial–mesenchymal transition [17–19]. However, our model employed a TNC Cre, localizing PAI-1 KD to resident renal fibroblasts [13]. Reduced fibroblast activation, shown by reduced TGF-β, CTGF and α-SMA expression

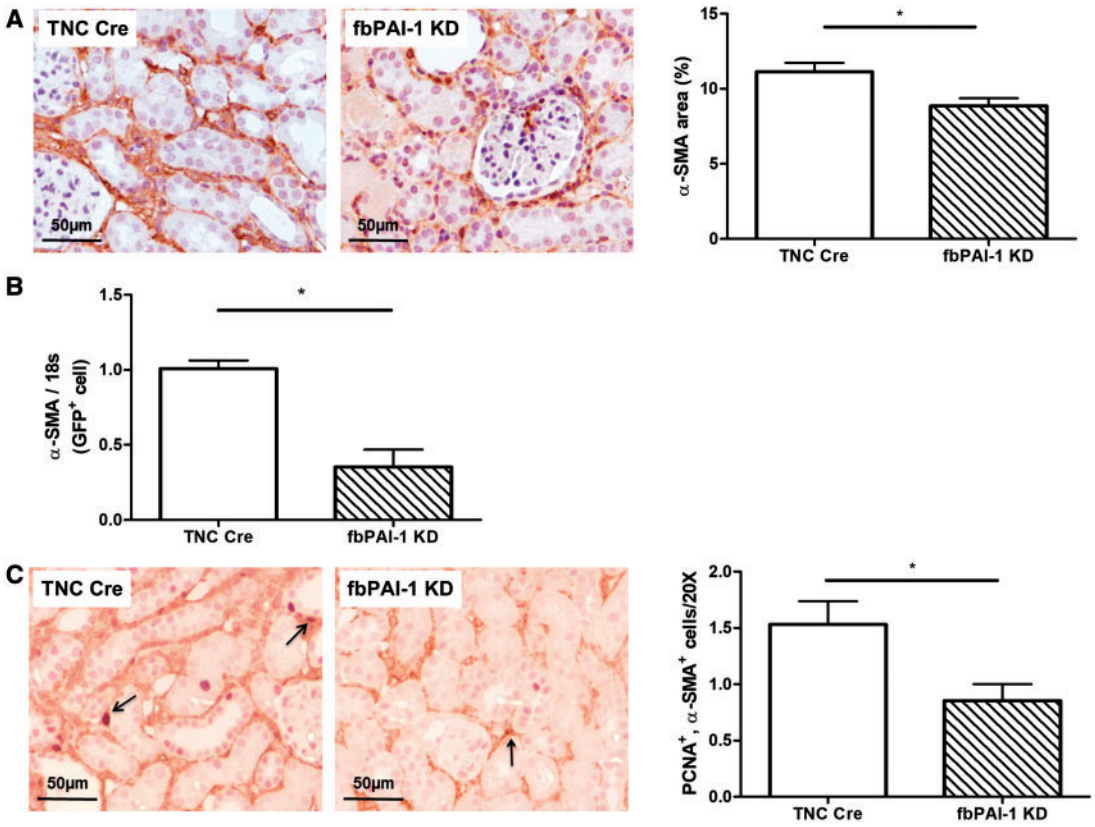


**FIGURE 3:** Fewer proliferating fibroblasts in fibroblast-specific PAI-1 KD mice. (**A**) Interstitial α-SMA$^+$ cells were significantly decreased in fbPAI-1 KD compared with TNC Cre (40×). (**B**) GFP$^+$ cells derived from fbPAI-1 KD kidneys showed less α-SMA expression. (**C**) Sections were double-stained with PCNA (purple) and α-SMA (brown). Fibroblast proliferation, assessed as double-stained cells (per 20× HPF), was decreased in fbPAI-1 KD versus TNC Cre. *$P < 0.05$.

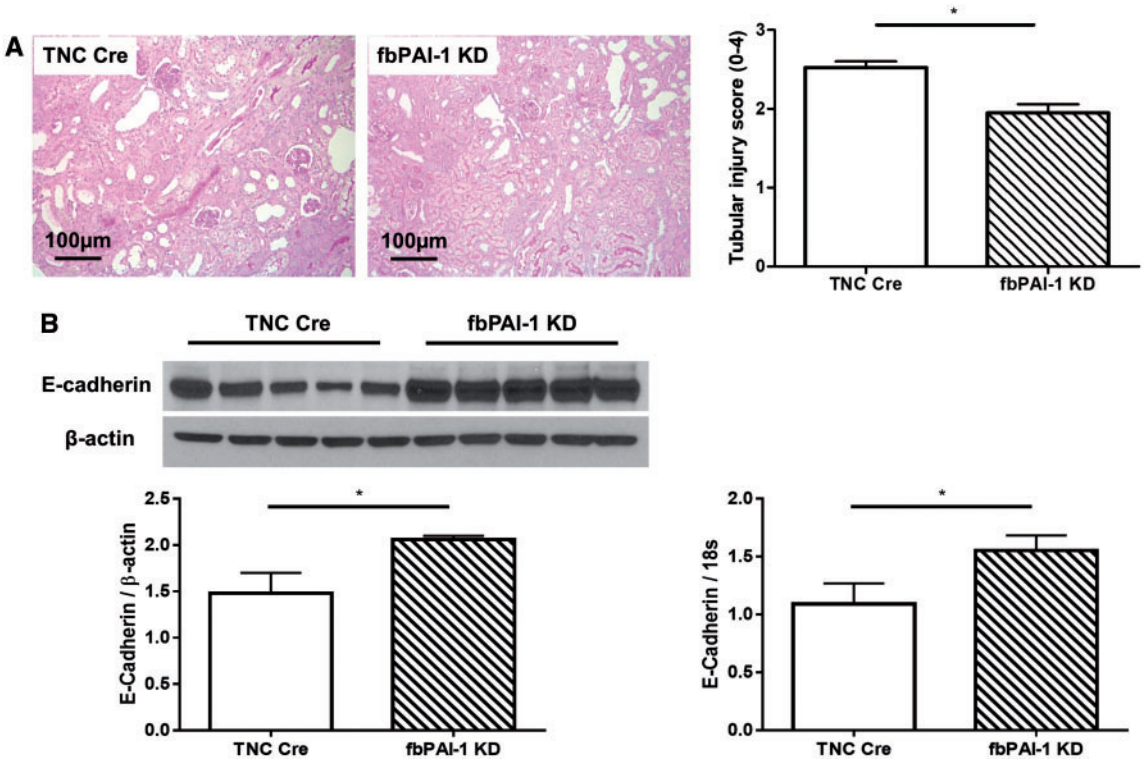


**FIGURE 4:** (**A**) fbPAI-1 KD mice showed less tubular injury than TNC Cre (periodic acid–Schiff, 20×). (**B**) E-cadherin mRNA and protein were preserved in fbPAI-1 KD compared with TNC Cre. *$P < 0.05$, **$P < 0.01$.

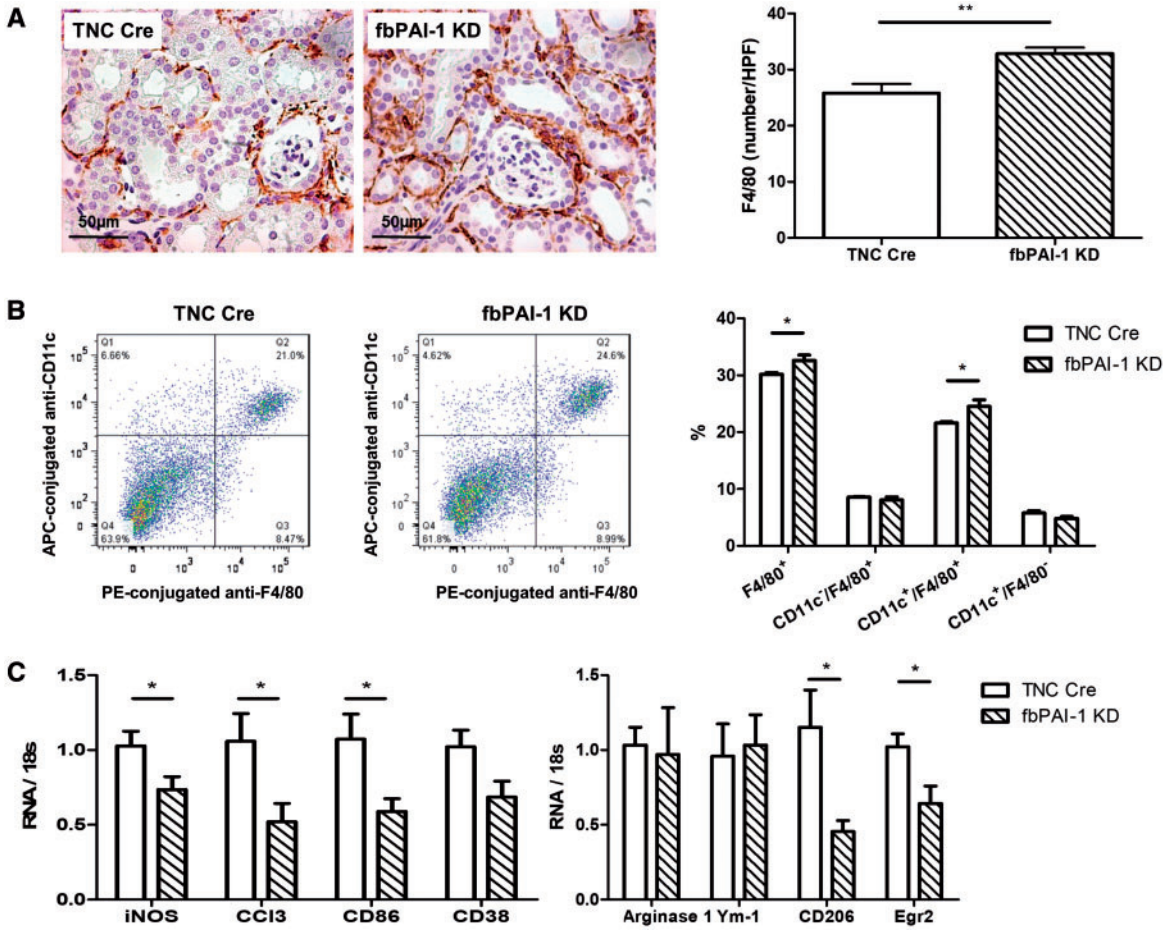


FIGURE 5: Increased F4/80$^+$ cell infiltration in fbPAI-1 KD mice. (**A**) Interstitial F4/80$^+$ cells were increased in fbPAI-1 KD compared with TNC Cre at Day 10 after UUO. (**B**) CD11c$^-$/F4/80$^+$ macrophages and CD11c$^+$/F4/80$^-$ dendritic cells were similar in fbPAI-1 KD and TNC Cre. CD11c$^+$/F4/80$^+$ cells were increased in fbPAI-1 KD mice compared with TNC Cre. (**C**) iNOS, Ccl3, CD86 and CD38, markers for M1 macrophages, were lower in CD11b$^+$ cells isolated from fbPAI-1 KD mice after UUO versus TNC Cre. CD206 and Egr2, M2 markers, were also reduced in fbPAI-1 KD kidneys after UUO, while two additional M2 markers (arginase-1 and Ym-1) showed no difference between the two groups. *$P < 0.05$, **$P < 0.01$.

in these cells, was linked to decreased fibroblast proliferation and less interstitial fibrosis in fbPAI-1 KD, suggesting that resident renal fibroblasts are a major mediator of PAI-1-mediated fibrosis. Of note, we have in previous studies shown in β6 integrin KD mice, which lack one significant pathway for activation of TGF-β through αvβ6 integrin, that PAI-1 can be increased and fibrosis induced, even in the absence of activated TGF-β, when additional angiotensin II or aldosterone was added to UUO injury in β6 knockout mice [20]. Thus overall TGF-β activation is not an obligate mediator of PAI-1 fibrotic effects. PAI-1 has been proven to promote the proliferation of cultured lung fibroblasts by activating $Ca^{2+}$, ERK and AKT signaling pathways [21]. The resulting decreased collagen may also interrupt a positive feedback cycle of increased matrix, promoting further fibroblast activation and proliferation. There may also be indirect antifibrotic effects of deleting PAI-1 in fibroblasts through preserved tubular epithelial cell differentiation, as shown by increased E-cadherin in the PAI-1 fibroblast KD kidneys compared with the injured TNC Cre mice with intact PAI-1 [22].

Depleting PAI-1 in fibroblasts increased F4/80$^+$ cell infiltration. Our data indicate that this is contributed to by CD11c$^+$/F4/80$^+$ macrophage/dendritic cells, while CD11c$^-$/F4/80$^+$ macrophages and CD11c$^+$/F4/80$^-$ dendritic cells did not change. Several previous studies suggested that CD11c$^+$ renal cells can function as antigen-presenting cells. However, one recent study indicated that CD11c$^+$/F4/80$^+$ cells were predominantly macrophages [23–26]. However, the previous study assessed the adriamycin nephropathy model, which results in primary glomerular and marked proteinuric injury with secondary tubulointerstitial fibrosis, quite different from the UUO model. It is possible that CD11c$^+$/F4/80$^+$ cells are composed of a mix of macrophages and dendritic cells. PAI-1 was hypothesized to function as a macrophage chemoattractant, supported by *in vitro* studies in which activated peritoneal macrophages had a chemotactic response to PAI-1 [10].

Polarization of macrophage subsets is a process governed by signaling molecules, inflammatory modulators and transcription factors [27, 28]. The M1 subset is proinflammatory, while M2 is considered profibrotic and wound-healing. Macrophage

plasticity is observed after UUO, with monocytes expressing high levels of Ly6C (indicative of M1 phenotype) recruited to the injured kidney postinjury, which then can remain Ly6C high or differentiate into a Ly6C medium- or low- (similar to M2) expressing phenotype [29]. PAI-1 expression is higher in M1 versus M2 macrophages from atherosclerotic patients [30]. Furthermore, conditional endothelium-specific PAI-1 deletion limited radiation-induced macrophage infiltration in the intestine with less M1 and more M2 than TNC Cre [31]. To further identify macrophage polarization and the influence of fibroblast PAI-1 KD on this process, we isolated $CD11b^+$ cells from the kidneys after UUO and found that these cells displayed reduced M1 markers, such as iNOS, Ccl3, CD86 and CD38 expression, in fbPAI-1 KD mice. The change of M2 markers, including reduced CD206 and Egr2, but with no change in arginase-1 and Ym-1, could be contributed to by different subtypes of $CD11b^+$ cells or different subtypes of M2 cells. Our study thus demonstrates that fibroblast PAI-1 KD was associated with altered macrophage recruitment and a reduced M1 phenotype shift. We therefore postulate that PAI-1 KD in renal fibroblasts affects the local immune and inflammatory milieu.

In summary, we found that depleting PAI-1 in fibroblasts ameliorates interstitial fibrosis with decreased fibroblast activation and proliferation. This is also associated with preserved tubular epithelial cell and reduced M1 macrophage markers.

## SUPPLEMENTARY DATA

Supplementary data are available at ndt online.

## FUNDING

This work was supported in part by the National Institues of Health National Institute of Diabetes and Digestive and Kidney Diseases (DK56942-09 to A.B.F.] and DK108968-01 to L.G.).

## AUTHORS' CONTRIBUTIONS

A.B.F. contributed to the conception and design. L.Y., L.S.P., A.M.K., J.Z. and HC.Y. contributed to experimentation and data acquisition. L.Y., M.F.W., L.S.P., J.Z., CM.H. and HC.Y. contributed to analysis and interpretation of the data. M.F.W., A.B.F., L.G., HC.Y. and A.B.F. provided writing or critical revision of the manuscript for important intellectual content. All authors approved the final version to be published.

## CONFLICT OF INTEREST STATEMENT

None declared.

## REFERENCES

1. Coresh J, Selvin E, Stevens LA *et al.* Prevalence of chronic kidney disease in the United States. *JAMA* 2007; 298: 2038–2047
2. Strutz F, Zeisberg M. Renal fibroblasts and myofibroblasts in chronic kidney disease. *J Am Soc Nephrol* 2006; 17: 2992–2998
3. Eddy AA, Fogo AB. Plasminogen activator inhibitor-1 in chronic kidney disease: evidence and mechanisms of action. *J Am Soc Nephrol* 2006; 17: 2999–3012
4. Keeton M, Eguchi Y, Sawdey M *et al.* Cellular localization of type 1 plasminogen activator inhibitor messenger RNA and protein in murine renal tissue. *Am J Pathol* 1993; 142: 59–70
5. Grandaliano G, Gesualdo L, Ranieri E *et al.* Tissue factor, plasminogen activator inhibitor-1, and thrombin receptor expression in human crescentic glomerulonephritis. *Am J Kidney Dis* 2000; 35: 726–738
6. Lee HS, Park SY, Moon KC *et al.* mRNA expression of urokinase and plasminogen activator inhibitor-1 in human crescentic glomerulonephritis. *Histopathology* 2001; 39: 203–209
7. Paueksakon P, Revelo MP, Ma LJ *et al.* Microangiopathic injury and augmented PAI-1 in human diabetic nephropathy. *Kidney Int* 2002; 61: 2142–2148
8. Nicholas SB, Aguiniga E, Ren Y *et al.* Plasminogen activator inhibitor-1 deficiency retards diabetic nephropathy. *Kidney Int* 2005; 67: 1297–1307
9. Gu C, Zhang J, Noble NA *et al.* An additive effect of anti-PAI-1 antibody to ACE inhibitor on slowing the progression of diabetic kidney disease. *Am J Physiol Renal Physiol* 2016; 311: F852–F863
10. Oda T, Jung YO, Kim HS *et al.* PAI-1 deficiency attenuates the fibrogenic response to ureteral obstruction. *Kidney Int* 2001; 60: 587–596
11. Matsuo S, Lopez-Guisa JM, Cai X *et al.* Multifunctionality of PAI-1 in fibrogenesis: evidence from obstructive nephropathy in PAI-1-overexpressing mice. *Kidney Int* 2005; 67: 2221–2238
12. He W, Xie Q, Wang Y *et al.* Generation of a tenascin-C-CreER2 knockin mouse line for conditional DNA recombination in renal medullary interstitial cells. *PLoS One* 2013; 8: e79839
13. Neelisetty S, Alford C, Reynolds K *et al.* Renal fibrosis is not reduced by blocking transforming growth factor-beta signaling in matrix-producing interstitial cells. *Kidney Int* 2015; 88: 503–514
14. Zhang MZ, Wang X, Wang Y *et al.* IL-4/IL-13-mediated polarization of renal macrophages/dendritic cells to an M2a phenotype is essential for recovery from acute kidney injury. *Kidney Int* 2017; 91: 375–386
15. Yang HC, Ma LJ, Ma J *et al.* Peroxisome proliferator-activated receptor-gamma agonist is protective in podocyte injury-associated sclerosis. *Kidney Int* 2006; 69: 1756–1764
16. Muzumdar MD, Tasic B, Miyamichi K *et al.* A global double-fluorescent Cre reporter mouse. *Genesis* 2007; 45: 593–605
17. Gomez IG, Duffield JS. The FOXD1 lineage of kidney perivascular cells and myofibroblasts: functions and responses to injury. *Kidney Int Suppl* 2014; 4: 26–33
18. LeBleu VS, Taduri G, O'Connell J *et al.* Origin and function of myofibroblasts in kidney fibrosis. *Nat Med* 2013; 19: 1047–1053
19. Grgic I, Duffield JS, Humphreys BD. The origin of interstitial myofibroblasts in chronic kidney disease. *Pediatr Nephrol* 2012; 27: 183–193
20. Ma LJ, Yang H, Gaspert A *et al.* Transforming growth factor-β-dependent and -independent pathways of induction of tubulointerstitial fibrosis in $\beta6^{-/-}$ mice. *Am J Pathol* 2003; 163: 1261–1273
21. Zhang YP, Wang WL, Liu J *et al.* Plasminogen activator inhibitor-1 promotes the proliferation and inhibits the apoptosis of pulmonary fibroblasts by $Ca^{2+}$ signaling. *Thromb Res* 2013; 131: 64–71
22. Loeffler I, Wolf G. Epithelial-to-mesenchymal transition in diabetic nephropathy: fact or fiction? *Cells* 2015; 4: 631–652
23. Kruger T, Benke D, Eitner F *et al.* Identification and functional characterization of dendritic cells in the healthy murine kidney and in experimental glomerulonephritis. *J Am Soc Nephrol* 2004; 15: 613–621
24. Dong X, Swaminathan S, Bachman LA *et al.* Antigen presentation by dendritic cells in renal lymph nodes is linked to systemic and local injury to the kidney. *Kidney Int* 2005; 68: 1096–1108
25. Brahler S, Zinselmeyer BH, Raju S *et al.* Opposing roles of dendritic cell subsets in experimental GN. *J Am Soc Nephrol* 2018; 29: 138–154
26. Cao Q, Wang Y, Wang XM *et al.* Renal $F4/80^+CD11c^+$ mononuclear phagocytes display phenotypic and functional characteristics of macrophages in health and in adriamycin nephropathy. *J Am Soc Nephrol* 2015; 26: 349–363
27. Wang N, Liang H, Zen K. Molecular mechanisms that influence the macrophage M1–M2 polarization balance. *Front Immunol* 2014; 5: 614
28. Rogers NM, Ferenbach DA, Isenberg JS *et al.* Dendritic cells and macrophages in the kidney: a spectrum of good and evil. *Nat Rev Nephrol* 2014; 10: 625–643

29. Lin SL, Castano AP, Nowlin BT *et al.* Bone marrow Ly6C$^{high}$ monocytes are selectively recruited to injured kidney and differentiate into functionally distinct populations. *J Immunol* 2009; 183: 6733–6743
30. Roma-Lavisse C, Tagzirt M, Zawadzki C *et al.* M1 and M2 macrophage proteolytic and angiogenic profile analysis in atherosclerotic patients reveals a distinctive profile in type 2 diabetes. *Diab Vasc Dis Res* 2015; 12: 279–289
31. Rannou E, Francois A, Toullec A *et al. In vivo* evidence for an endothelium-dependent mechanism in radiation-induced normal tissue injury. *Sci Rep* 2015; 5: 15738

*Received: 18.4.2018; Editorial decision: 20.2.2019*